Electronic Supplementary Material (ESI) for Nanoscale
This journal is © Royal Society of Chemistry 2019

Supplementary Information

Metal-Organic Framework Derived 3D Graphene Decorated $NaTi_2(PO_4)_3$ for Fast Na-ion Storage

Lei Wang [a,b], Zhennan Huang [b], Bo Wang [a,*], Hao Luo [a], Meng Cheng [b], Yifei Yuan [b], Kun He [b], Tara Foroozan [b], Ramasubramonian Deivanayagam [b], Guijing Liu [c], Dianlong Wang [a,*], and Reza Shahbazian-Yassar [b,*]

[a] *MIIT Key Laboratory of Critical Materials Technology for New Energy Conversion and Storage, School of Chemistry and Chemical Engineering, Harbin Institute of Technology, 150001 Harbin, China.*

[b] *Department of Mechanical and Industrial Engineering, University of Illinois at Chicago (UIC), Chicago, IL 60607, USA*

[c] *School of Chemistry and Materials Science, Ludong University, Yantai, 264025, P R China*

∗ *Corresponding author. Fax: +86 45186413721; Tel: +86 45186413751.*

E-mail address:

wangbo19880804@163.com (B. Wang),

wangdianlonghit@163.com (D. L. Wang),

rsyassar@uic.edu (R. S. Yassar).

Calculation Methods: The specific capacity of electrode materials was calculated from galvanostatic charge-discharge (GCD) tests according to the equations S1, where S*C* is the specific capacity, *I* is the discharge current, Δt is the discharge time, and *m* is the mass loading of active materials (for example, the mass of NTP-rGO composites includes the mass of NTP and rGO), respectively.

$$SC = \frac{I\Delta t}{m} \qquad \text{(S1)}$$

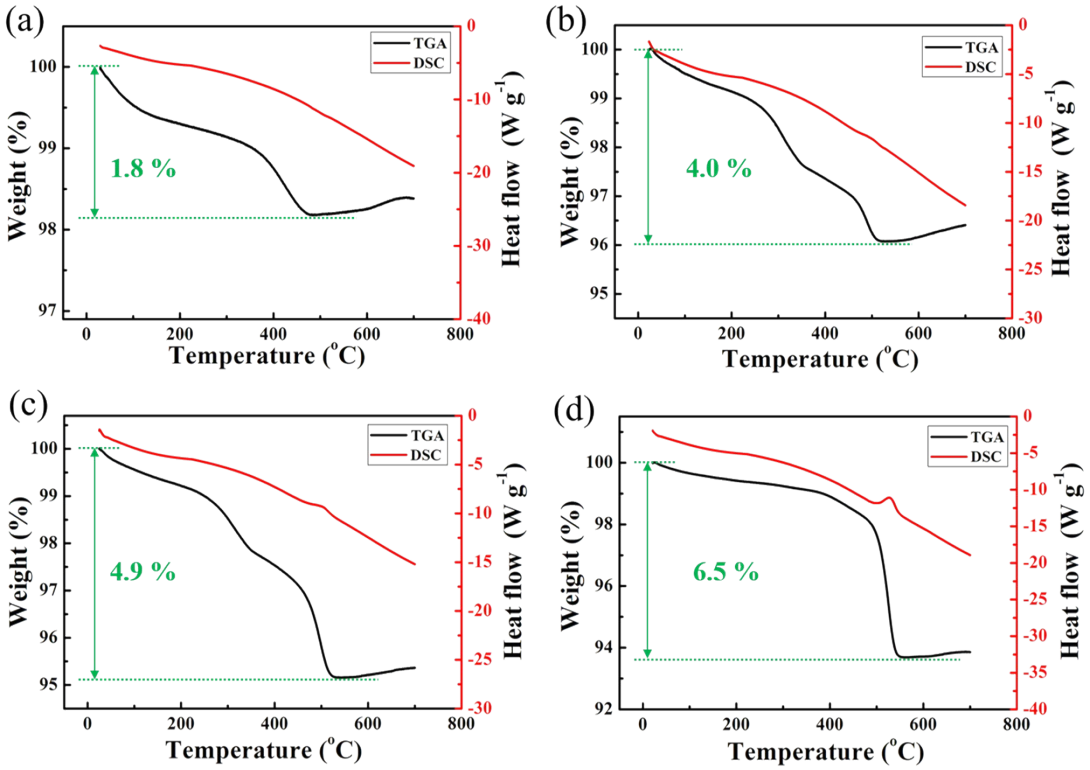

Fig. S1† TGA/DSC curves of all samples (a) NTP, (b) NTP-rGO-10, (c) NTP-rGO and (d) NTP-rGO-30.

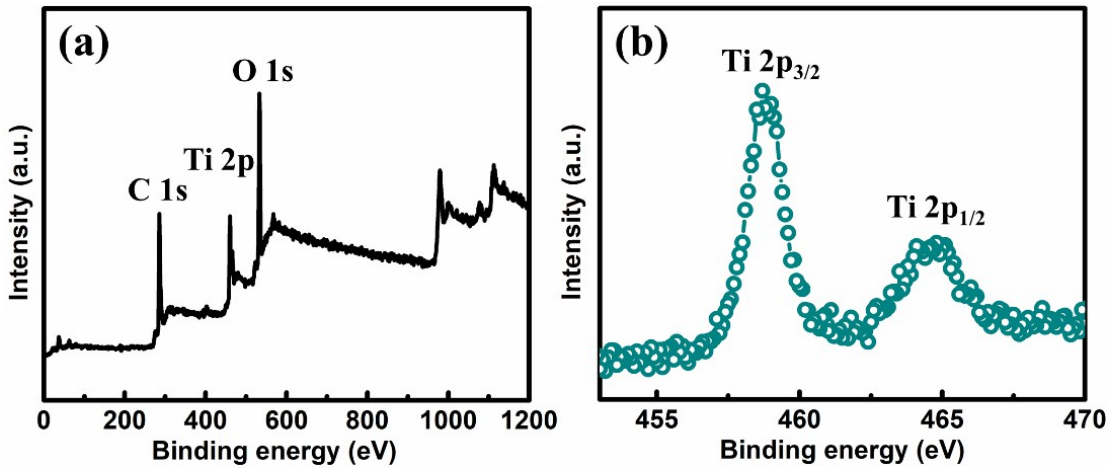

Fig. S2† XPS survey spectrum of MIL-125 and the corresponding high-resolution Ti 2p XPS spectrum.

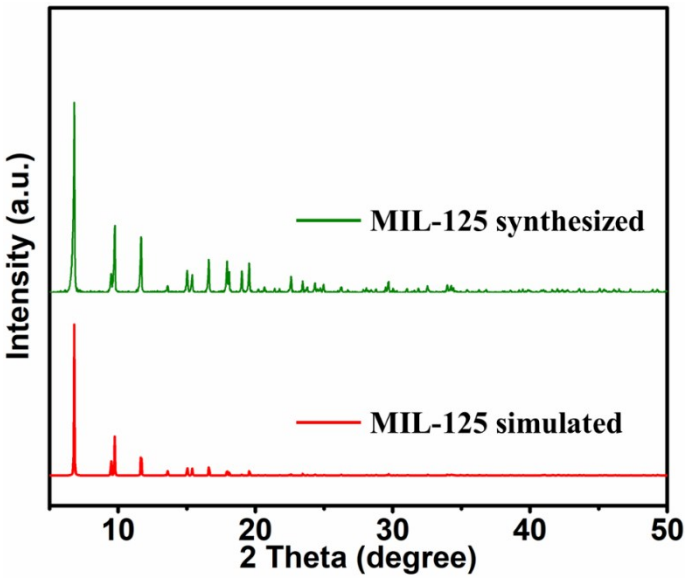

Fig. S3† XRD pattern of MIL-125 compared with the MIL-125 simulated.

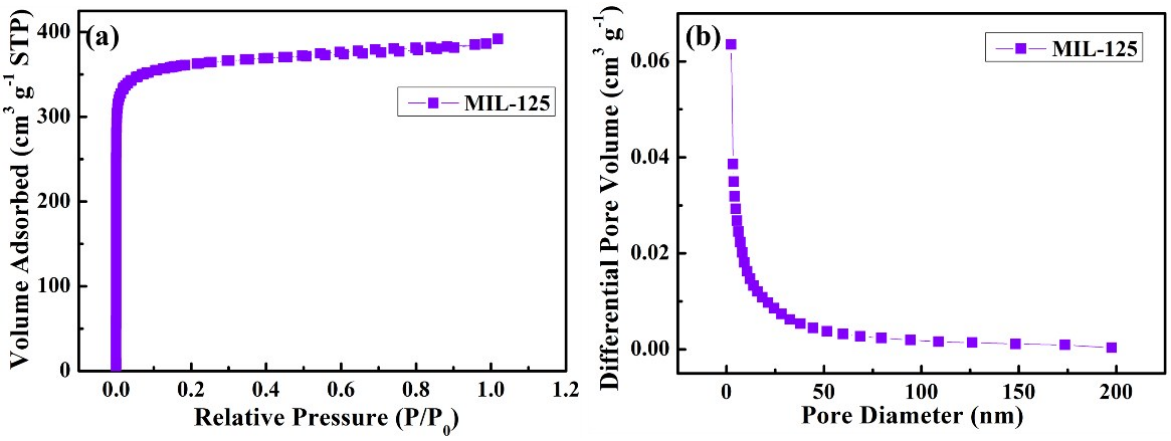

Fig. S4† (a) Nitrogen adsorption-desorption isotherms of MIL-125; (b) The pore size distribution plot of MIL-125

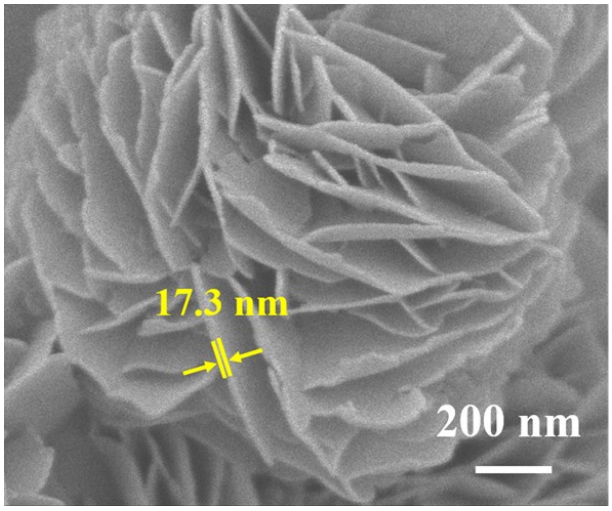

Fig. S5† SEM image of the NTP precursor.

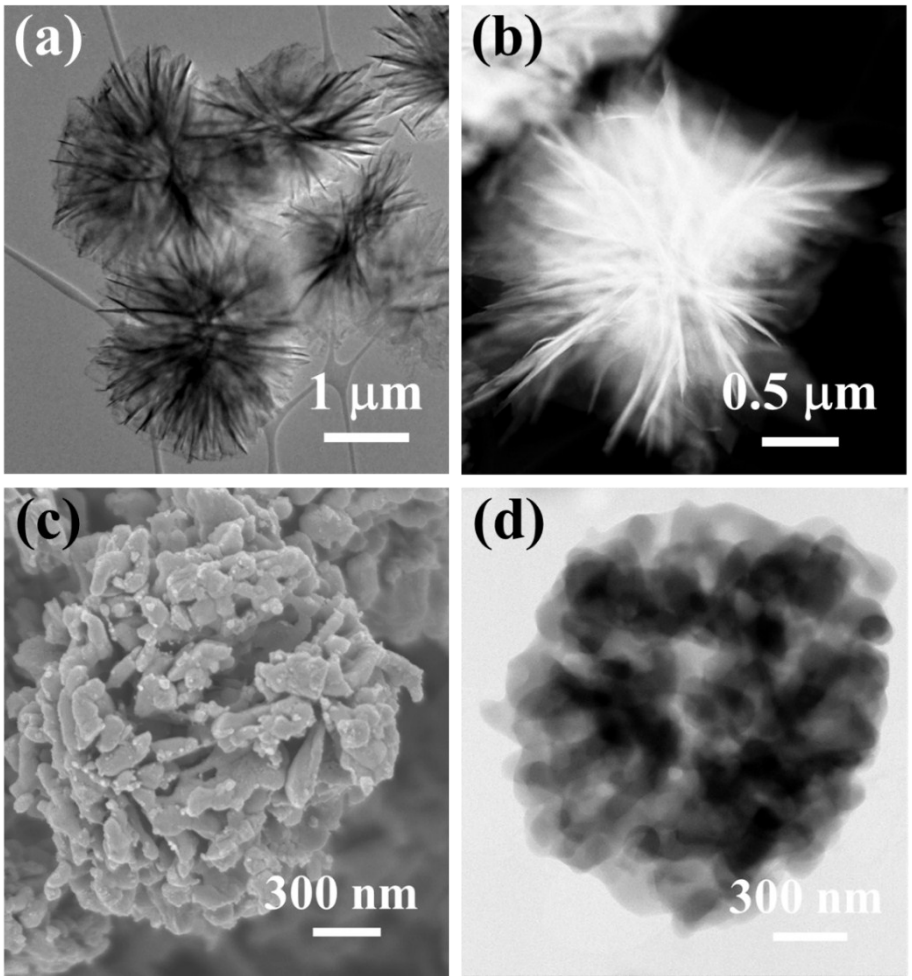

Fig. S6† TEM images of (a) NTP precursor and (b) NTP-rGO precursor; (c) SEM image of NTP; (d) TEM image of NTP sample.

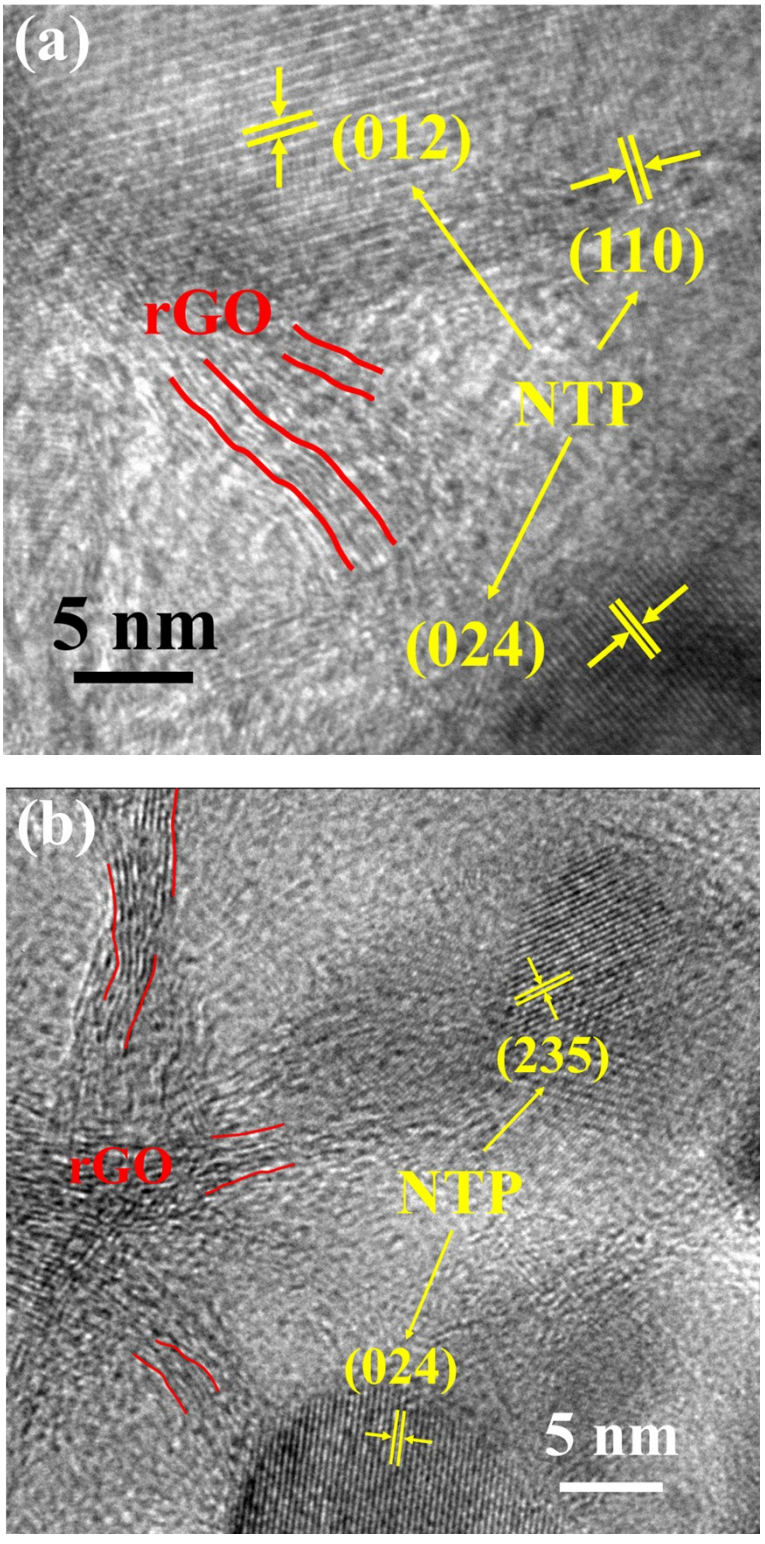

Fig. S7† HRTEM image of the NTP-rGO.

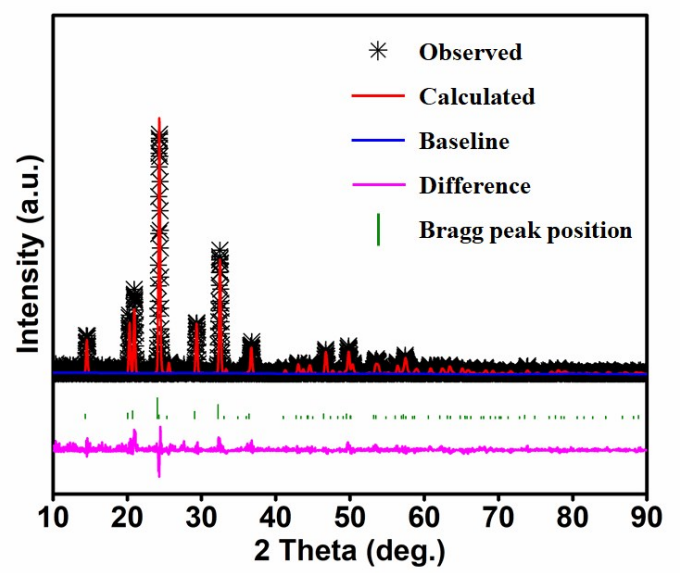

Fig. S8† XRD pattern of the NTP-rGO and its Rietveld refinement.

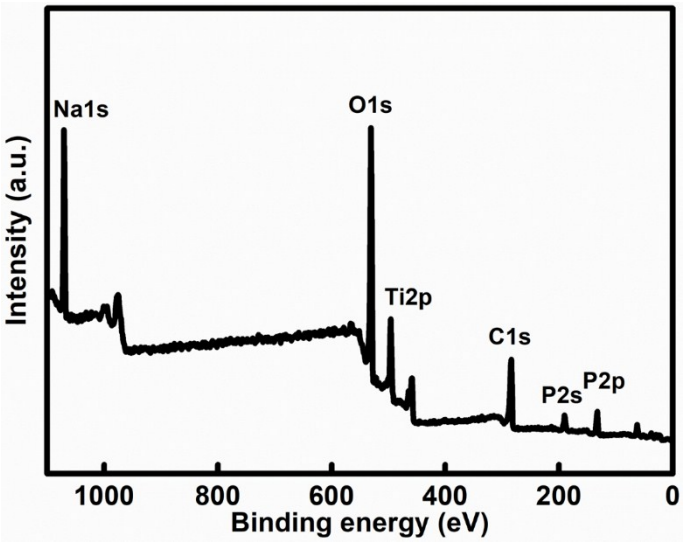

Fig. S9† XPS survey spectrum of the NTP-rGO.

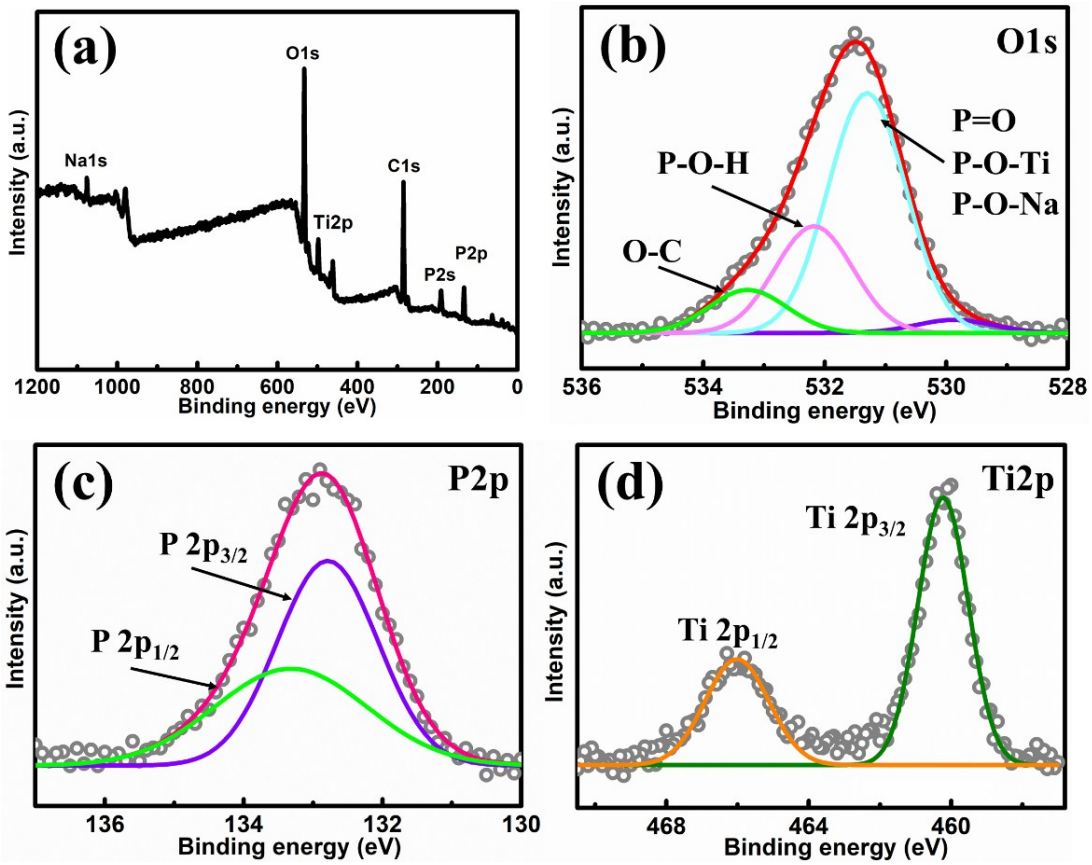

Fig. S10† (a) XPS survey spectrum of the NTP and high-resolution spectra for (b) O 1s, (c) P 2p and (d) Ti 2p, respectively.

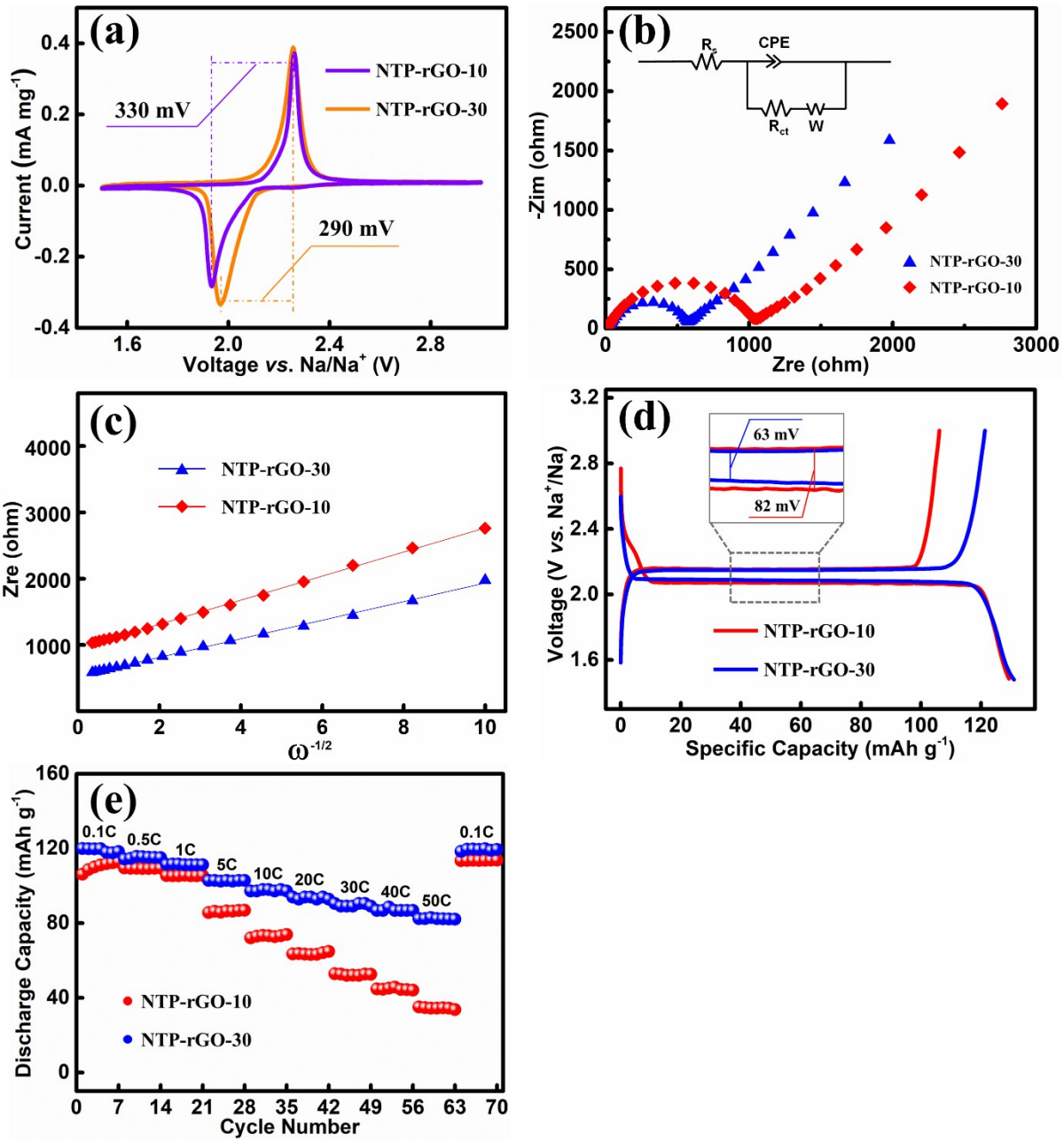

Fig. S11† The electrochemical performance of NTP-rGO-10 and NTP-rGO-30. (a) CV curves. (b) Nyquist plots and the equivalent circuit (the inset). (c) The relationship between Z_{re} and $\omega^{-1/2}$ at low frequency from EIS test. (d) The first cycle of the discharge-charge curves. (e) Rate performance.

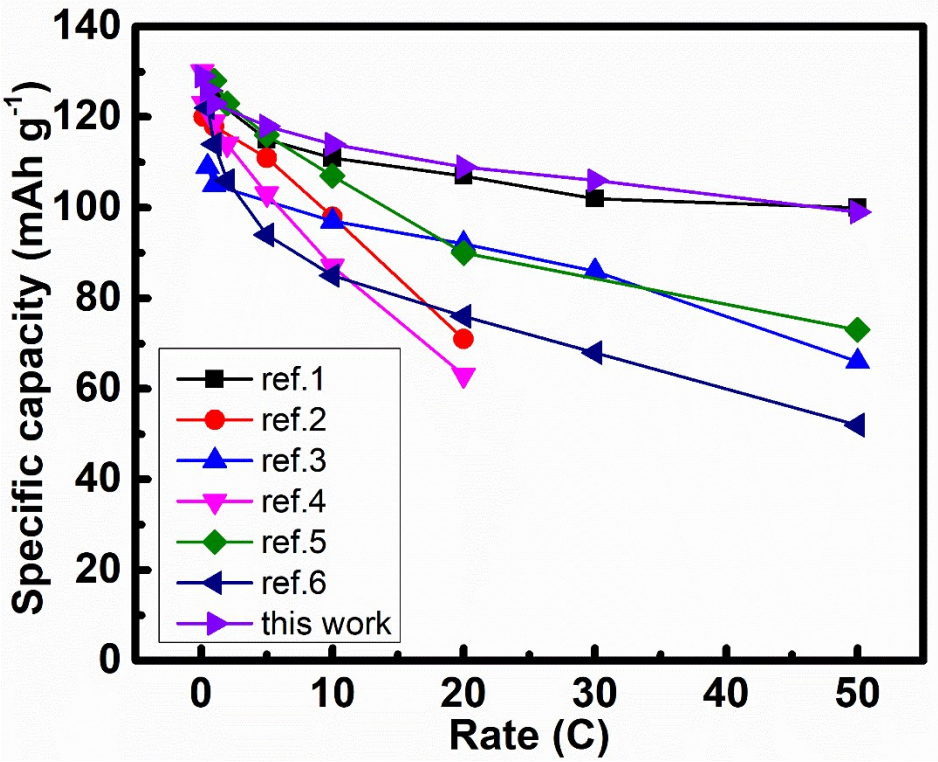

Fig. S12† The comparison of specific capacity and rate capability of NTP-rGO in this work with others published recently. [1-6]

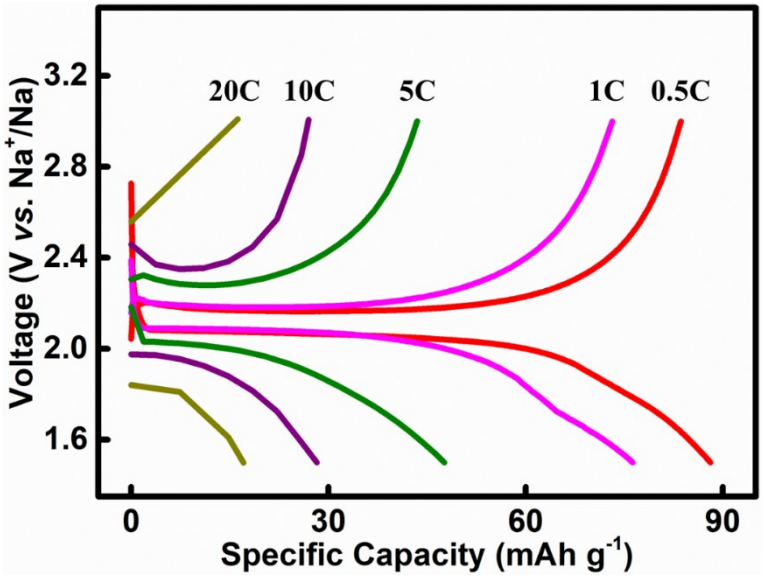

Fig. S13† The discharge-charge curves of NTP electrode at various current densities.

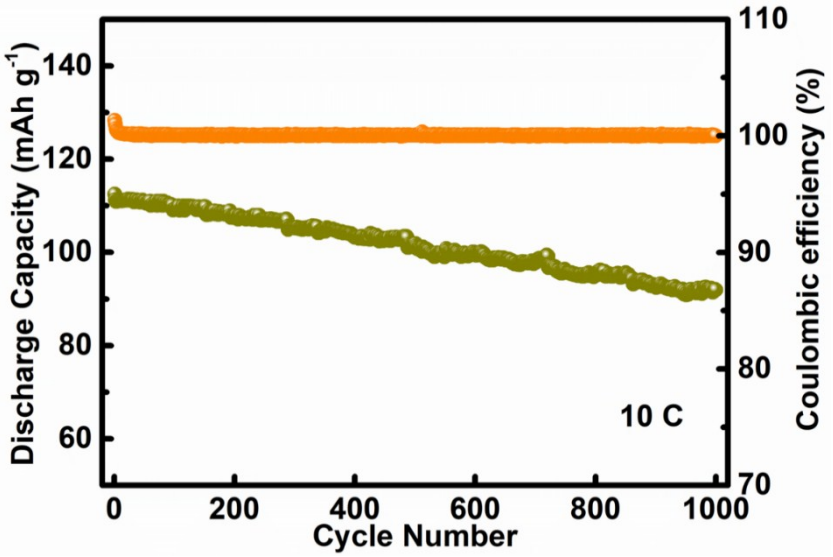

Fig. S14† Cycling stability test at 10 C for NTP-rGO electrode.

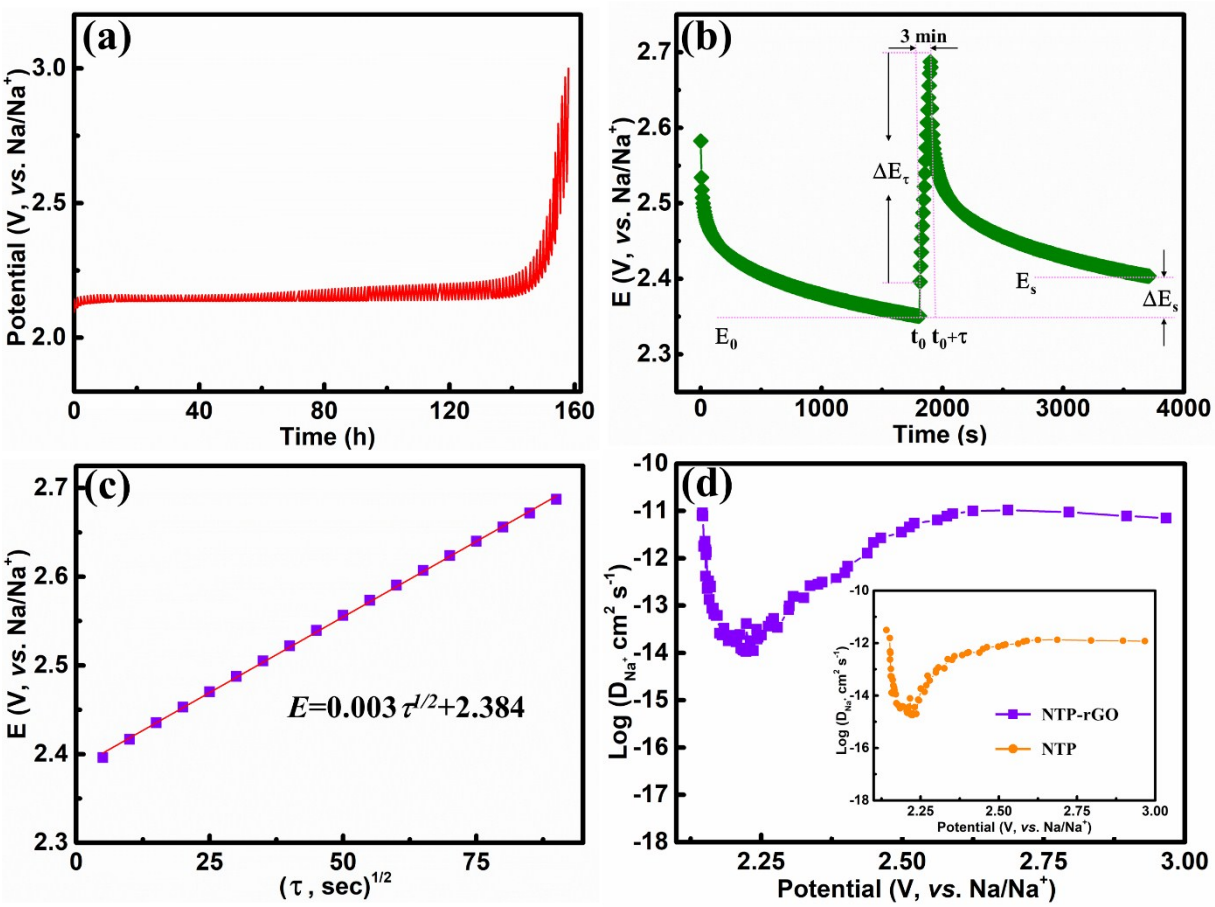

Fig. S15† (a) The charge GITT curves of NTP-rGO. (b) *t* vs. *E* profile for a single GITT titration. (c) Linear behavior of *E* vs. $\tau^{1/2}$ relationship. (d) The calculated D_{Na+} from GITT data for the NTP-rGO electrode and the NTP electrode (the inset).

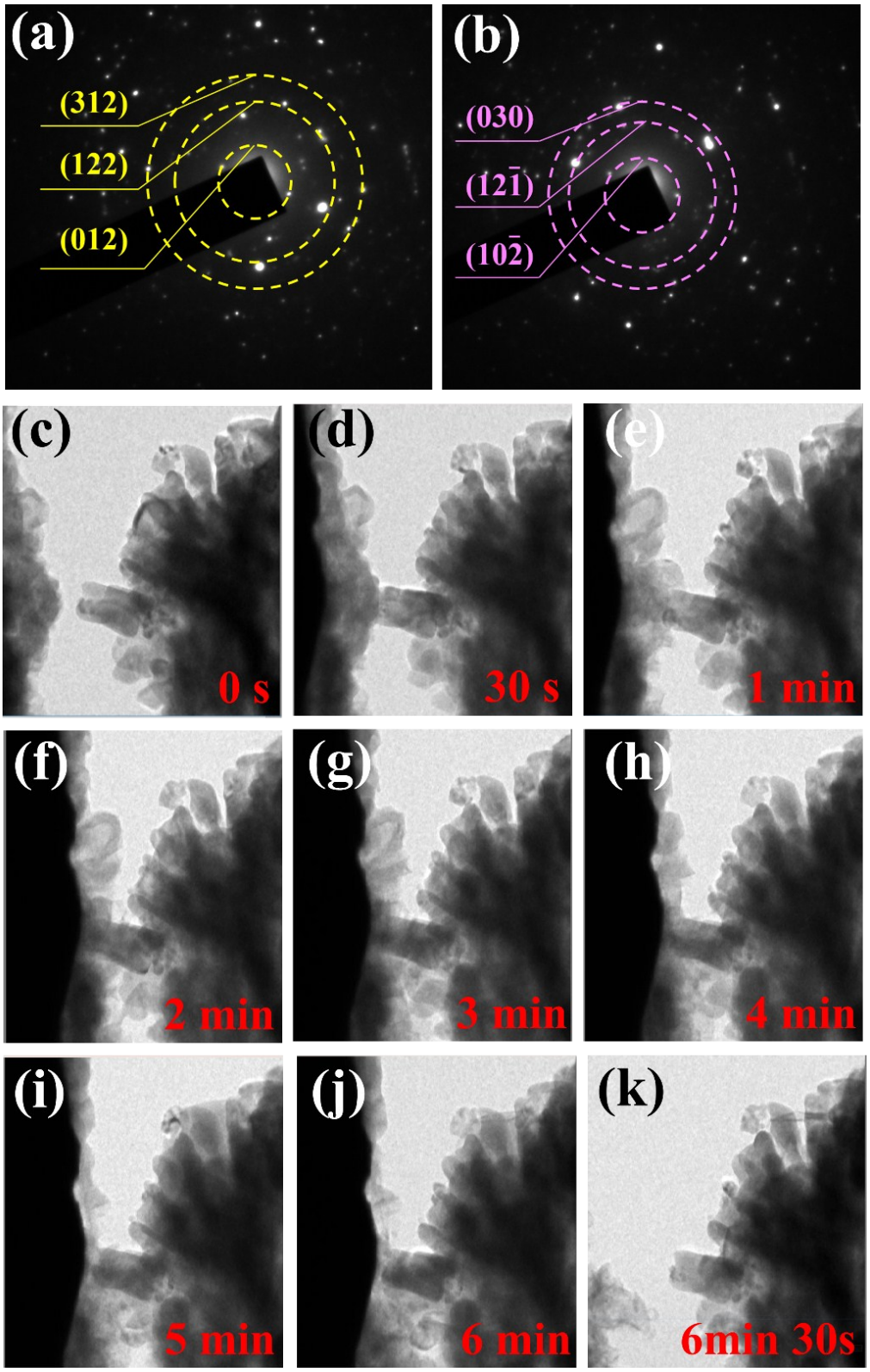

Fig. S16† SAED pattern of the NTP a) before sodiation and b) after sodiation. c-k) *In-situ* TEM of the NTP during the sodiation/desodiation process.

Table S1 The comparison of CE of NTP-rGO in this work with recent published works.

Materials	Current density (C)	Coulombic efficiency (%)	Ref.
This work	0.1 C	96.8%	-
NTP⊂GN	1 C	79%	[7]
NTP@C@PC	1 C	95%	[8]
NTP-NBA	1 C	83%	[9]
NTP⊂rGO-CNTs	1 C	90%	[5]
NTP/C P2	0.1 C	95%	[10]
h-MNTP/WMCNTs	0.5 C	96.6%	[11]

Reference

1. C. Xu, Y. Xu, C. Tang, Q. Wei, J. Meng, L. Huang, L. Zhou, G. Zhang, L. He and L. Mai, *Nano Energy*, 2016, *28*, 224-231.
2. P. Wei, Y. Liu, Z. Wang, Y. Huang, Y. Jin, Y. Liu, S. Sun, Y. Qiu, J. Peng, Y. Xu, X. Sun, C. Fang, J. Han and Y. Huang, *ACS Appl. Mater. Inter.*, 2018, *10*, 27039-27046.
3. L. Fu, X. Xue, Y. Tang, D. Sun, H. Xie and H. Wang, *Electrochim. Acta*, 2018, *289*, 21-28.
4. M. Li, L. Liu, P. Wang, J. Li, Q. Leng and G. Cao, *Electrochim. Acta*, 2017, *252*, 523-531.
5. G. Xu, Z. Li, X. Wei, L. Yang and P. K. Chu, *Electrochim. Acta*, 2017, *254*, 328-336.
6. L. Xu, G. Xu, Z. Chen, X. Wei, J. Cao and L. Yang, *J. Mater. Sci.: Materials in Electronics*, 2018, *29*, 9258-9267.
7. C. Wu, P. Kopold, Y. Ding, P. Aken, J. Maier, Y. Yu, *ACS Nano*, 2015, *9*, 6610.
8. Y. Jiang, L. Zeng, J. Wang, W. Li, F. Pan and Y. Yu, *Nanoscale*, 2015, *7*, 14723-14729.
9. G. Yang, H. Song, M. Wu and C. Wang, *J. Mater. Chem. A*, 2015, *3*, 18718-18726.
10. Z. Huang, L. Liu, L. Yi, W. Xiao, M. Li, Q. Zhou, G. Guo, X. Chen, H. Shu, X. Yang and X. Wang, *J. Power Sources*, 2016, *325*, 474-481.
11. G. B. Xu, L. W. Yang, X. L. Wei, J. W. Ding, J. X. Zhong and P. K. Chu, *J. Power Sources*, 2016, *327*, 580-590.